03.1;03.2

Collisions of liquid droplets and solid particles in a heated gaseous medium

© A.G. Islamova, P.P. Tkachenko, N.E. Shlegel, P.A. Strizhak

Tomsk Polytechnic University, Tomsk, Russia
E-mail: agi2@tpu.ru

Received February 15, 2024
Revised March 22, 2024
Accepted March 28, 2024

The paper presents experimental data on the characteristics of collisions between water suspension droplets and sand particles in a gaseous medium at different initial temperatures. Typical interaction modes (agglomeration, separation) were established. The interaction mode map has been drawn taking into account simultaneous contributions of the inertia, surface tension, and viscosity forces. There were determined conditions for intense fragmentation of liquid droplets, as well as for stable agglomeration of droplets and particles during which suspension droplets get formed. The study has shown that an increase in the temperature of the gaseous medium from 20 to Fx0xEC leads to a 30% shift of the boundary between the agglomeration and separation modes towards lower Weber numbers. This was assumed to occur because of changes in the liquidś physical properties (viscosity decrease by 30%, surface tension decrease by up to 10%).

Keywords: collision, agglomeration, separation, particle, droplet.

DOI: 10.61011/TPL.2024.07.58728.19893

Collisions between liquid droplets play an important role in many engineering and research applications: in the fuel, chemical, irrigation and food industries [1]. Those collisions determine key production process parameters, such as droplet size distribution, degree of mixing, evaporation rate and heat transfer, which affect the efficiency and reliability of the processes involved in this phenomenon [2]. Several modes of collisions between droplets and solid particles are possible: agglomeration, recoil and destruction [3,4]. Initiation of these modes depends on such factors as droplet and particle characteristics (size and geometry), properties of fluids, environmental conditions [5]. An actual task is formation of particles having the required size, properties and surface shapes by thermal drying [6]. The method of thermal drying is performed using slurry reactors in which the suspension droplets collide with solid particles [7]. The main advantage of this method is the possibility of obtaining solid particles with the required functional and properties, such as flowability, behavior in recovery, bulk density and mechanical stability [8]. There are known results of studies [3,4] which considered collisions of droplets of impurity-free liquids, as well as of droplets of solutions, with regular-shaped particles under normal conditions. In practice, particles are asymmetric and nonuniform, and the temperature of their interaction with liquid droplets is considerably higher than that corresponding to normal conditions. Papers [7–9] devoted to investigating interaction between liquid droplets and solid particles in sprays pay attention mainly to integral parameters (mean size, humidity). This paper presents characteristics of the processes of droplet/solid particle interaction. The goal of this study is to determine from experimental results characteristics of the droplet/particle interaction in the gaseous medium with varying temperature of the latter.

Fig. 1 presents a schematic diagram of the test bench used to study droplet/particle collisions in the gaseous medium; the main interaction characteristics to be measured are also shown. The droplet/particle collisions were detected using a highspeed video camera (resolution of 1280×1024 px, shooting speed of 5000 fps, interframe delay of 1/25 000 s). Solid particles were fed into the collision chamber by using a sandblasting gun with a reservoir. Fraction size of sand particles was below 1 mm. Sand was ground in a rotary mill. The rotor speed varied from 60 to 20 000 rpm depending on the fraction desired to be obtained. Ground sand was sifted with a vibrating screen. To spray the particles, the sandblasting gun was equipped with a compressor. To vary the particle motion speed, the compressor was set to the pressure of 2–6 atm. Liquid droplets were generated with a booster connected to the compressor. By varying the pressure from 2 to 6 atm, the droplet motion speed and size were varied. As the test fluid, a water-sand suspension was used (95 wt.% of water, 5 wt.% of sand). This ratio was chosen taking into account operating conditions and performance characteristics of the dryers [10]. The suspension components were mixed in a magnetic mixer at 950 rpm for 10 min. After that, the suspension was fed into the reactor. Sand particles had no time to sediment and remained suspended in droplets. The gaseous medium temperature varied from 20 to 100°C.

In the course of highspeed video recording, the following main parameters of the droplet/particle interaction were fixed: radii of droplets (R_d) and particles (R_p), speeds of droplets (U_d) and particles (U_p), angle between the dropletsánd a particlesťrajectories (α_d), distance between

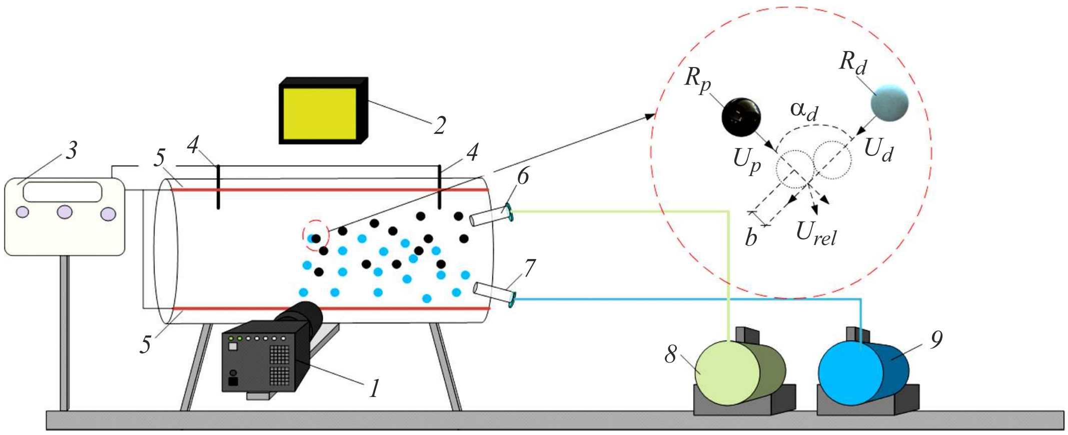

Figure 1. Test bench for measuring characteristics of collisions between the liquid and solid-particle flows. *1* — video camera, *2* — projector, *3* — control panel, *4* — thermocouples, *5* — heaters, *6* — feed nozzle for the solid particles, *7* — feed nozzle for the liquid, *8* — compressor feeding the solid particles, *9* — compressor feeding the liquid.

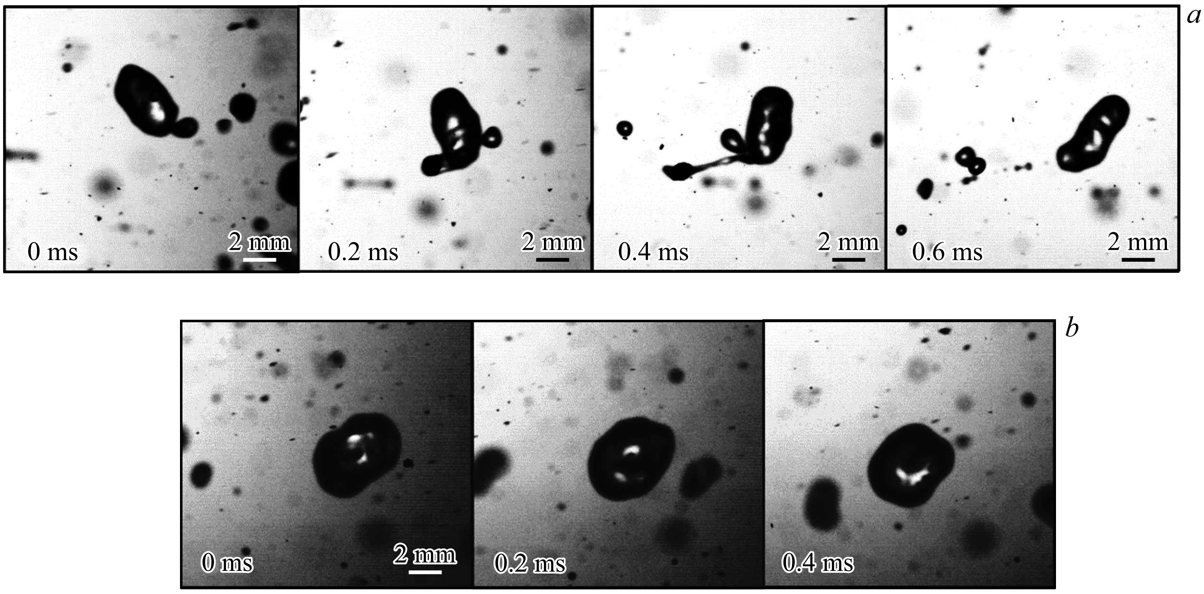

Figure 2. Photos illustrating collisions of water droplets with a particle in the aerosol flow. *a* — agglomeration, *b* — separation.

the particle and droplet centers of mass (b). The systematic measurement errors of the droplet sizes, motion speeds, and collision angles were 2, 4 and 2%, respectively. Based on the measurements, the resulting rate of the droplet/particle interaction $U_{rel} = (U_d^2 + U_p^2 - 2\cos(\alpha_d)U_dU_p)^{0.5}$ was calculated. In the course of analyzing the video records, the Weber number was calculated as $\mathrm{We} = 2\rho R_d U_{rel}^2/\sigma$. Linear interaction parameter $B = b/(R_d + R_p)$ was also calculated. Parameter B may vary from zero to unity.

In analyzing the experimental results, two modes of interaction between the suspension droplets and sand particles were identified: agglomeration and separation (Fig. 2). Regularities of these modes are described in detail in [11]. Realization of the agglomeration mode was observed at relatively low resulting motion speeds (below 2 m/s). A sand particle settled on a suspension droplet; no secondary fragments were formed. When the resulting interaction rate or sizes of droplets and particles increased, a transition between the agglomeration and separation modes occurred. In the mode of separation, formation of secondary fragments took place.

Based on the results of analyzing video records obtained in the conducted experiments, a conclusion was made that the droplet/particle size ratio has a decisive effect on the droplet/particle collision modes and consequences. The fact was established that the smaller is the initial droplet size, the smaller is the number of secondary fragments being formed during collisions. It was found out that grinding of small droplets needs lower resulting collision rates. And, vice versa, an increase in the initial droplet size was accompanied by an increase in the resulting motion speeds necessary for droplet separation. In line with this,

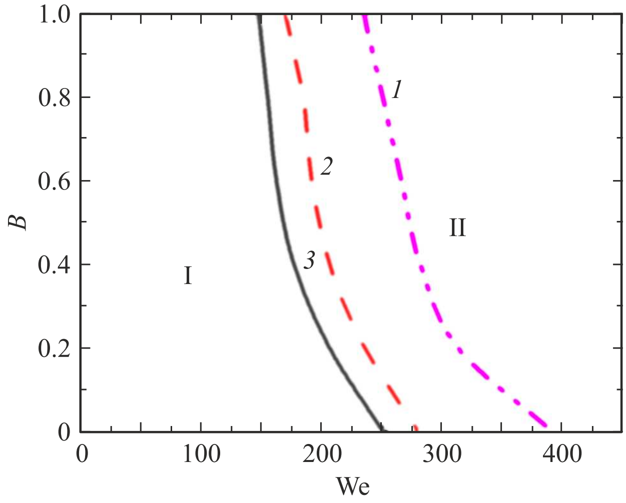

Figure 3. A map of the liquid droplet/solid particle collision modes for different ambient temperatures: 20 (*1*), 50 (*2*) and 100°C (*3*). I — agglomeration, II — separation.

an increase in the droplet size led to an increase in the Weber number necessary for the separation mode. This was because when the droplet was larger than the particle, and their motion speeds were the same, the droplet pulled the particle inside itself. As the motion speeds of particles and droplets increased, their fragmentation was observed. It was also shown that, when the droplet and particle relative concentration increased from $2 \cdot 10^{-4}$ to $6 \cdot 10^{-4}$, the probability of the separation mode increased by 10–15%. This was caused by droplet surface deformation due to frequent collisions with neighboring particles and droplets. Each subsequent impact of a particle on such a droplet resulted in its grinding.

Based on the experimental results, a map of modes of the suspension droplet/solid sand particle collisions in aerosol flows was constructed (Fig. 3).

In constructing the mode map, there was used dimensionless linear interaction parameter B which enabled accounting for the droplet and particle radii, as well as the collision centricity. The Weber number allowed accounting for the forces of inertia and surface tension, as well as for contributions of the droplet motion speed and size. What was also established was that, when the gaseous medium temperature increased to 100°C, the process of droplet separation proceeds stably at Weber numbers 20–30% lower than at the ambient temperature of 20°C. This effect is associated with the fact that droplets warmed up in the gaseous medium. When the liquid was heated, the film surface tension forces decreased, and its destruction needed lower initial droplet speeds and, hence, lower interaction energies. Temperatures in the working chamber were determined with thermocouples and thermal imaging camera (Fig. 1). The assessment performed showed that liquid droplets have time to warm up to 40–60°C while moving from the nozzle to the collision zone. In this case, surface tension decreased from 72.69 to 66.37 mN/m, while viscosity decreased from 1.0 to 0.7 mPa·s. Intensification of the droplet separation was also promoted by the presence of solid particles in it. A decrease in the liquid surface tension led to a decrease in the drag force inside the droplet, which affects the suspension particles. At the moment of impact, particles „broke“ the droplet near-surface layers from inside due to the predominance of inertia forces over the surface tension forces. An increase in the gaseous medium temperature reduced also the external drag; the droplet/particle interaction rates were higher than those under normal conditions. This effect initiated an increase in the number of secondary fragments arising during droplet separation. The experiments have shown that an increase in the gaseous medium temperature promoted reduction in the secondary fragment size. This is because of intensification of phase transitions.

In the range of gaseous temperatures under study, no vapor buffer zone was observed during collisions between suspension droplets and solid particles. Paper [12] has shown that when the gaseous medium temperature increases above 400°C, the buffer vapor zone gets formed around the droplet. It prevents the droplets from approaching each other and intensifies their repulsion caused by oppositely directed water-vapor flows from droplet surfaces. When the gaseous medium temperatures vary in the range of 20–100°C, the boundaries between the droplet collision modes shown in the map depend on the influence of thermal conditions on the properties of fluids.

Funding

The study was supported by the Russian Science Foundation, project № 23-71-10040 (https://rscf.ru/project/23-71-10040/).

Conflict of interests

The authors declare that they have no conflict of interests.

References

[1] Yu.D. Chashechkin, V.E. Prokhorov, Tech. Phys., **68** (11), 1431 (2023).
[2] S. Suo, M. Jia, H. Liu, T. Wang, Int. J. Multiphase Flow, **137**, 103581 (2021). DOI: 10.1016/j.ijmultiphaseflow.2021.103581
[3] H. Kan, H. Nakamura, S. Watano, Adv. Powder Technol., **29**, 1317 (2018). DOI: 10.1016/j.apt.2018.02.026
[4] G.V. Kuznetsov, P.A. Strizhak, Tech. Phys. Lett., **45** (3), 267 (2019). DOI: 10.1134/S1063785019030301.
[5] D. Pan, N. Phan-Thien, B.C. Khoo, J. Non-Newton. Fluid Mech., **212**, 63 (2014). DOI: 10.1016/j.jnnfm.2014.08.011
[6] H. Yang, A. Chen, S. Geng, J. Cheng, F. Gao, Q. Huang, C. Yang, Chin. J. Chem. Eng., **44**, 51 (2022). DOI: 10.1016/j.cjche.2021.03.045
[7] I. Malgarinos, N. Nikolopoulos, M. Gavaises, Fuel Process. Technol., **156**, 317 (2017). DOI: 10.1016/J.FUPROC.2016.09.014

[8] N.M. Eijkelboom, A.P. van Boven, I. Siemons, P.F.C. Wilms, R.M. Boom, R. Kohlus, M.A.I. Schutyser, J. Food Eng., **337**, 111222 (2023). DOI: 10.1016/j.jfoodeng.2022.111222
[9] V.A. Arkhipov, S.A. Basalaev, A.I. Konovalenko, K.G. Perfil'eva, Tech. Phys. Lett., **46** (6), 610 (2020). DOI: 10.1134/S1063785020060176.
[10] *Handbook of non-ferrous metal powders*, ed. by O.D. Neikov, S.S. Naboychenko, N.A. Yefimov (Elsevier, Oxford, 2019), p. 621. DOI: 10.1016/B978-0-08-100543-9.00014-2
[11] S.K. Pawar, F. Henrikson, G. Finotello, J.T. Padding, N.G. Deen, A. Jongsma, F. Innings, J.A.M.H. Kuipers, Powder Technol., **300**, 157 (2016). DOI: 10.1016/j.powtec.2016.06.005
[12] A.V. Demidovich, S.S. Kralinova, P.P. Tkachenko, N.E. Shlegel, R.S. Volkov, Energies, **12**, 4256 (2019). DOI: 10.3390/en12224256

Translated by EgoTranslating